SIMULATIONS INVESTIGATING COMBINED EFFECT OF LATERAL AND VERTICAL NAVIGATION ERRORS ON PBN TO XLS TRANSITION

David De Smedt, Emilien Robert, EUROCONTROL, Brussels, Belgium

Ferdinand Behrend, Technical University Berlin, Berlin, Germany

Abstract

Building further on previous PBN to precision final approach transition work (PBN to xLS), EUROCONTROL in collaboration with the Technical University of Berlin (TUB) and under the SESAR[1] work programme, conducted an experiment investigating the combined lateral and vertical performance of 5 different aircraft types when transitioning from a curved PBN procedure to a precision final approach procedure (using an ILS, GLS or more generically an xLS landing system). While earlier work has concentrated primarily on either lateral or vertical performance during these operations, the current work focusses on the combined lateral and vertical transition aspects. Arinc 424 procedures, consisting of a 180 degree turn using the Radius-To-Fix path terminator, connected to either a 3NM or a 6NM Final Approach Segment were implemented in 5 different aircraft simulators of the following types: A340, B777, B737, E190 and Dash8Q400. To test the procedures under the most realistic conditions, simulated lateral navigation errors ranging between -0.15NM and 0.15NM were introduced in the PBN segments of each procedure, while non-standard temperatures ranging between ISA-37 and ISA+35 were implemented in the simulator. Besides the effect of the lateral navigation errors on the xLS transition already studied in the previous work, the additional effects of deviations in the vertical profile caused by the non-standard temperatures were investigated. Also, a number of scenarios were added to the test cases which contained steeper glide paths with angles up to 4 degrees. Conclusions were formulated regarding the different aircraft capabilities and performances, as well as flight crew considerations. The overall conclusion of this work is that it is possible for all investigated aircraft to transition directly from a curved PBN procedure to an xLS procedure without the requirement of an intermediate segment between final approach course and glide path interception. This is true under the conditions that the glide path is intercepted at a certain distance from the threshold and from a PBN segment containing a defined vertical path which is significantly shallower than the glide path. Additionally, final approach course and glide path capture will require flight crew interventions other than just arming the approach mode in certain situations, i.e. high above ISA temperature deviations and lateral navigation errors. The final objective of this work is to progress to a set of procedure design criteria which would enable the design and publication of PBN to xLS procedures.

Introduction

Research has been conducted during the previous years, investigating modern aircraft's capabilities to fly curved paths over the ground using advanced PBN functions like the Radius-to-Fix (RF) function. Using the RF capability, as specified by current aviation standards [1], a curved path over ground with a defined constant radius can be flown between a defined start and end point. Aircraft equipped with this function will adjust the bank angle during the turn, in function of groundspeed and specified turn radius, to stay on track. Tracking performance of systems using the RF function was assessed in earlier work [2] [3].

In parallel, certain work packages under the SESAR work programme investigated the possibility to conduct advanced approach and landing procedures using Ground Based augmentation Systems (GBAS). More in particular, SESAR work package 6.8.8 considers the following three potential scenarios for improved approach and landing operations [4]:

- Increased glideslopes (including adaptive and double glideslopes)

[1] Single European Sky ATM Research

- Multiple runway aiming points
- Curved precision approach (RNP to xLS)

Earlier research work [5] presented at the 33rd DASC concentrated on the last bullet point: RNP to xLS, where RNP refers to the part of the route flown using the aircraft's Flight Management System (FMS) with the RNP specification according to the Performance Based Navigation (PBN) Manual [6]. xLS refers to the final approach (ILS, MLS or GLS) during which steering navigation is provided by the Multi-Mode Receiver (MMR). The work presented in [5] focused on the lateral aircraft performance when transitioning from RNP to xLS flight modes: scenarios consisting of a 180 degree turn using the Radius to Fix (RF) path terminator, connected to respectively a 3, 6 and 9NM final xLS segment, were flown in 6 different full motion flight crew training simulators (A340, A320, B777, B737, E190 and Dash-8 Q400). The scenarios were designed such that the end of the RF turn coincided with the Final Approach Point (FAP) of the xLS procedure, such that both the final approach course (localizer in case of an ILS) and glide path could be intercepted simultaneously at this point. While flying the procedures, simulated lateral navigation errors of up to 0.3NM were introduced in the simulation. The conclusion was that final approach course intercept behavior was very much dependent on the aircraft type and the installed avionics. Depending on the introduced lateral navigation bias, some aircraft could or could not automatically intercept the final approach course at the end of the turn. In some aircraft, a flight crew intervention was always necessary switching to a basic "heading hold" flight mode, before the final approach mode could be armed and the final approach course intercepted. In order to at least ensure that the aircraft was within final approach course (localizer) full scale range at the end of the RF turn, the following relation was proposed between allowed maximum horizontal position uncertainty y, distance from FAP to threshold x, distance from localizer transmitter to threshold d_{loc} and localizer full range angular beam width θ:

$$y = (x + d_{loc}) \cdot \tan(0.5 \cdot \theta) \qquad (1)$$

Additionally [5] concluded that, when the design is such that localizer and glide path are intercepted at the same point i.e. the Final Approach Point (FAP), 5NM is a good value for the minimum distance of this Final Approach Point to the threshold. This allowed the aircraft to be fully stabilized at 3NM before the threshold.

While [5] investigated mainly lateral PBN to xLS transition issues, a related study [7] focused on the vertical performance by conducting similar PBN to xLS simulations on a wide range of avionics test benches and aircraft simulators. The latter simulations were performed under non-standard temperature conditions, ranging from ISA -48C to ISA +35C. These temperature variations have an influence on the aircraft's altitude: in lower than standard temperature conditions, the true altitude of the aircraft will be lower than the indicated altitude while in higher than standard temperature conditions, the true altitude will be higher than the indicated altitude. Obviously this will have an effect when transitioning from the PBN procedure, during which a vertical path is flown using barometric guidance, to the xLS procedure during which vertical guidance is provided by using the xLS glide path. The simulations in [7] where flown without any assumed lateral navigation error. It was concluded that a continuously descending path definition for these procedures would be problematic operationally as for above ISA deviations, captures necessarily would be from above while for below ISA deviations capture problems where observed with the aircraft descending below the FAP altitude. Therefore in [7], incorporation of a shallower segment, defined by an "AT" altitude constraint prior to the FAP and approximately aligned with the final approach course is recommended. Note that the procedures in [7] were flown assuming a 3 degree barometric descent angle along the PBN procedure, transitioning to a 3 degree glide angle at the FAP.

Simulation Setup

Purpose of the simulation

The purpose of the simulation presented in this paper was to test the combined effect of lateral navigation errors and temperature deviations on the transition from a curved PBN procedure (using the Radius to Fix function) to an xLS final approach procedure. As already mentioned in [5], procedure design criteria are currently defined in [8] for

conventional xLS procedures and for procedures using RF legs in the intermediate segments of RNP approaches with vertical guidance (APV Baro or APV SBAS). For RF to xLS transitions, no specific design criteria other than the conventional criteria for xLS procedures are specified. Conventional criteria require an intermediate segment between 1.5 and 2NM aligned with the final approach course, to permit the aircraft to stabilize and establish on the final approach course prior to intercepting the glide path. This simulation investigates whether it is possible to connect the RF segment directly to the Final Approach Point (FAP) of the xLS procedure without the intermediate segment, thus allowing localizer and glide path interception at the same point. Furthermore, the objective of the simulation was to confirm the minimum distance to the threshold at which an RF leg could connect to the final approach, taking into account lateral navigation errors combined with non-standard temperatures affecting the vertical transition. Lateral navigation errors introduced in the simulations were either 0, +/- 0.1 or +/- 0.15NM, putting the aircraft right (positive error) or left (negative error) of the localizer centerline while approaching clockwise the end of the RF leg. Temperature deviations were between ISA-37 and ISA+35 degrees Celsius.

A second objective of the simulation was to test the aircraft's capability to fly the same procedures with steep xLS glide paths as proposed by SESAR WP 6.8.8. Glide path angles of up to 4.5 degrees are considered in [4], although the ICAO PANS-OPS procedure design criteria [8] recommend 3 degrees and prescribe a minimum of 2.5 and a maximum of 3.5 degrees for CAT I precision (ILS/MLS/GBAS) approaches (maximum of 3 degrees for CAT II/III). Any steeper angle is subject to an aeronautical study and requires special approval by the national competent authority. For R&D purposes and to support the work described in [4], the xLS glide paths in some of the simulation scenarios were increased to 4 degrees, including one scenario with a 4.5 degree glide path. These scenarios were flown using the same range of lateral navigation errors and temperature offsets as for the procedures with standard glide paths.

Procedure design

The same procedures and databases were used as in [5]. As illustrated in figure 1, three different procedures were developed consisting of an RF leg with radii of respectively 1.5, 2.3 and 2.8NM, connected directly to the Final Approach Point at respectively 3, 6 and 9NM from the threshold. The glide path angles of the final xLS segments were configured in the simulator before each scenario (usually 3 degrees or higher for the steep approaches). Altitude constraints were associated to the start and end points of the RF leg in order to achieve a curved segment with a defined vertical path angle (usually 2 degrees). Additionally, speed constraints of respectively 180, 200 and 220kts were associated to the start point of each RF leg, ending respectively at a 3, 6 or 9NM Final Approach Point. All procedures were coded in Arinc 424 format using the latest Arinc 424 specification [9] and converted into loadable databases by the avionics manufacturers. Figure 1 provides a general overview of the different procedures, while Figure 2 illustrates one of the implemented procedures visualized on the Navigation Display in one of the simulators.

As in [5], the lateral navigation errors during the PBN procedure were simulated by laterally shifting the procedure coded in the aircraft's navigation database by a value equal to the assumed navigation error while the xLS final approach segment remained fixed in the simulation. Temperature offsets were entered directly on the instructor's panel in the simulator. The entry of these temperature offsets turned out to be non-obvious, as explained further in detail in the next chapter discussing the effect of temperature on the aircraft's altitude.

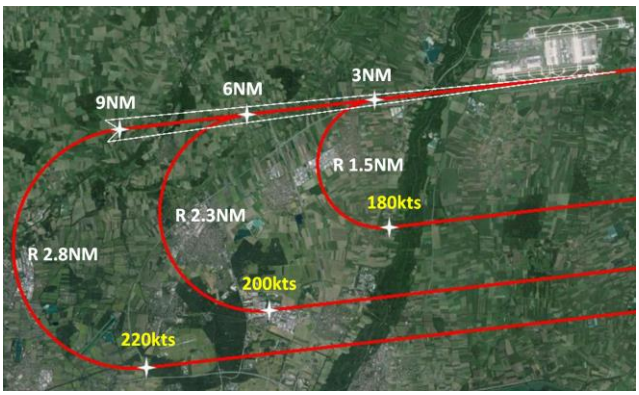

Figure 1. Overview of Designed Procedures

Figure 2. Navigation Display with Radius-To-Fix Procedure and Vertical Path

Test Facilities

The simulators used in the test series were five full motion flight simulators operated by Lufthansa Flight Training and Swiss Aviation Training. They all have the highest certification standard called JAR-STD 1A Level D which is normally used for flight crew training. More in particular, the following aircraft simulator types were used:

- Boeing B737-300
- Boeing B777-200
- Airbus A340-300
- Embraer E190
- Bombardier Q400

The flight characteristics of the simulators correspond to existing reference aircraft to ensure a realistic behavior of the whole aircraft system. The simulators were equipped with original avionics, including the original Flight Management System (FMS). Custom databases containing the full set of designed procedures were provided by Honeywell, GE Aviation and Universal Avionics and loaded in the corresponding FMSs of the simulators. The simulators were equipped with a motion system with six degrees of freedom and a 180 degree wide visual system. An example of the interior of the simulators is provided in Figures 3 to 7.

A possibility was given during the test series to modify the glideslope angle using inputs to the maintenance computer which is located in the flight compartment of the full flight simulator. Therefore, the required value has to be entered into the common database via an interface normally used for monitoring purposes by the maintenance staff. The common database is a shared memory used for all operations of the running simulation processes. It contains all parameters (labels) of the simulation process and can be modified by inserting specific values. If the label representing the current glideslope angle is changed manually the simulated glideslope beam takes the inserted value as long no other ILS frequency is inserted into the radio management panel of the respective aircraft. If so, it changes automatically the value for the glideslope angle corresponding to the stored ILS frequency in the FMS. However, the functionality for manipulating specific glideslope angle values provides the possibility to use every desired value of glideslope angle at any time for every selected ILS-equipped runway.

Figure 3. Airbus A340 Flight Simulator

Figure 4. Boeing 737 Flight Simulator

Figure 5. Boeing B777 Flight Simulator

Figure 6. Embraer 190 Flight Simulator

Figure 7. Bombardier Q400 Flight Simulator

Data Recording

A Data Gathering Utility (DGU) was installed on the simulation host computer in order to create log files of the simulation state as stored in the system memory. It scans a specified set of up to 200 labels at regular intervals (up to 60 Hz) and writes the values into the log file for subsequent evaluation purposes. This type of data recording was available for 3 out of 5 simulator types. High-definition video recordings of the Primary Flight Display (PFD) and the Navigation Display (ND) were made for each scenario during the tests in all 5 simulator types.

Effect of temperature on aircraft altitude

Temperature deviations were entered directly via the instructor's panel in the simulator. The management of these temperature profiles in the simulator turned out to be non-obvious, due to the following two reasons:

- Temperature profiles in the simulator were usually obtained by adjusting the temperature at airport level, after repositioning the aircraft. A lag in response time of the actual temperature profile in the simulator was often observed, after this temperature modification.
- The temperature profile was often affected by a previous temperature entry at an

altitude above airport level which was not automatically adjusted.

Because of the above, although the desired ISA deviation before each simulation run was entered correctly and consistently in the simulator at airport elevation, the temperature profiles during the simulations showed both an ISA offset at airport elevation and a non-ISA temperature lapse rate (slope of the temperature profile with altitude). Figure 8 illustrates the temperature profiles which were implemented during the simulations runs, after post analysis of the data.

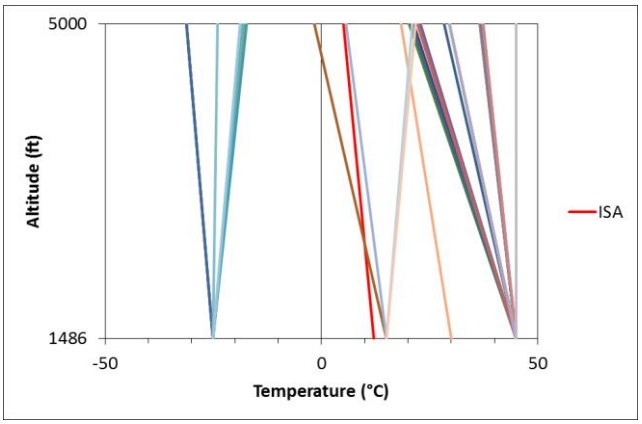

Figure 8. Temperature Profiles Versus altitude for Each Scenario (ISA Temperature Profile in Red)

Therefore, in order to perform a correct evaluation of the influence of temperature on the aircraft performance, it was decided to undertake a detailed theoretical study, investigating the effect on the aircraft's true altitude of temperature profiles with an offset ground temperature and a non-standard temperature lapse rate. This is further discussed in the next two paragraphs.

Effect of temperature profile with constant ISA deviation and standard temperature lapse rate

Formulas relating the geopotential height of the aircraft to the pressure height, in function of an ISA deviation which is constant with altitude, could be found in [8], [10] and [11]. However two of those references contained an error in the formula. Actually, at the time of writing this paper, the only reference which contains a correct version of the formula is ICAO PANS-OPS Volume II, in which the formula is presented as follows [8]:

$$\Delta h_{correction} = \Delta h_{PAirplane} - \Delta h_{GAirplane}$$

$$\Delta h_{correction} = -\frac{\Delta ISA}{\lambda} \cdot \ln\left(1 + \frac{\lambda \cdot \Delta h_{PAirplane}}{T_0 + \lambda \cdot h_{PAerodrome}}\right) \quad (2)$$

With:

$\Delta h_{PAirplane}$ = Aircraft height above aerodrome (pressure)

$\Delta h_{GAirplane}$ = Aircraft height above aerodrome (geopotential)

ΔISA = temperature deviation from the standard day (ISA) temperature

λ = standard temperature lapse rate with pressure altitude in the first layer (sea level to tropopause) of the ISA

T_o = standard temperature at sea level

$h_{PAerodrome}$ = aerodrome elevation

Note that this formula is not valid in case of temperature deviations with a non-standard temperature lapse rate. For non-standard temperature lapse rates, PANS-OPS Volume II refers to another document [12] however a copy of this document could not be obtained at the time of writing. Therefore a complete mathematical derivation of a formula relating geopotential height to pressure height for temperature profiles with non-standard temperature lapse rates and non-standard pressures at sea level is given in the next paragraph.

Effect of temperature profile with ISA deviation on ground and non-standard temperature lapse rate

Formulas relating pressure to height originate from the following hydrostatic fluid equation:

$$dp = -\rho \cdot g \cdot dh_g \quad (3)$$

With:

p = pressure at height above ground h_g

ρ = air density

g = gravitational constant ($9.81 m/s^2$)

h_g = geopotential height above ground (airport)

If the atmosphere is considered as an ideal gas, the following addition relation applies:

$$p = \rho \cdot R \cdot T \tag{4}$$

With:

R = specific gas constant ($287 m^2/s^2/K$)

T = temperature at pressure p

Combining formulas (3) and (4) yields:

$$\frac{dp}{p} = -\frac{g}{RT} \cdot dh_g \tag{5}$$

Integrating formula (5) yields:

$$-\frac{R}{g} \cdot \ln\left(\frac{p}{p_a}\right) = \int_0^{h_g} \frac{1}{T} \cdot dh_g$$

$$-\frac{R}{g} \cdot \left[\ln\left(\frac{p}{p_0}\right) - \ln\left(\frac{p_a}{p_0}\right)\right] = \int_0^{h_g} \frac{1}{T} \cdot dh_g \tag{6}$$

With:

p_a = pressure at airport elevation

p_0 = standard pressure at sea level (1013.25 hPa)

Below the tropopause (11000m), a standard aircraft altimeter will measure pressure p and convert this to a pressure altitude h above 1013 hPa, using the following relation defined for the International Standard Atmosphere [13] [14]:

$$\frac{p}{p_0} = \left(\frac{T_{ISA}}{T_0}\right)^{-\frac{g}{\lambda R}} = \left(\frac{T_0 + \lambda h}{T_0}\right)^{-\frac{g}{\lambda R}} \tag{7}$$

With:

T_0 = standard temp. at sea level (288.15 °K)

λ = standard temp. lapse rate (-0.0065 °K/m)

h = pressure height above 1013.25 hPa

Substituting (7) in (6) yields:

$$\frac{1}{\lambda} \cdot \ln\left(\frac{T_0 + \lambda h}{T_0}\right) + \frac{R}{g} \ln\left(\frac{p_a}{p_0}\right) = \int_0^{h_g} \frac{1}{T} \cdot dh_g \tag{8}$$

Note that if the pressure p_a at the airport is the standard pressure $p_{a,ISA}$ ($p_a = p_{a,ISA}$), formula (7) in which p is replaced by $p_{a,ISA}$ and h is replaced by the airport elevation h_a, can be substituted in the left side of equation (8), which yields:

$$\frac{1}{\lambda} \cdot \ln\left(\frac{T_{a,ISA} + \lambda(h - h_a)}{T_0}\right) - \frac{1}{\lambda} \ln\left(\frac{T_{a,ISA}}{T_0}\right) = \int_0^{h_g} \frac{1}{T} \cdot dh_g$$

$$\frac{1}{\lambda} \cdot \ln\left(1 + \frac{\lambda(h - h_a)}{T_{a,ISA}}\right) = \int_0^{h_g} \frac{1}{T} \cdot dh_g \tag{9}$$

With:

h_a = airport elevation

$T_{a,ISA}$ = standard temperature at airport elevation

If we assume that T is constant ($T=T_c$; temperature above airport is not varying with height), then (9) can be integrated as follows:

$$h_g = \frac{T_c}{\lambda} \cdot \ln\left(1 + \frac{\lambda(h - h_a)}{T_{a,ISA}}\right) \tag{10}$$

If we subsequently substitute T_c in equation (10) with an average ISA temperature T_{ISA} and an average ISA temperature T_{ISA} + constant ISA deviation ΔISA, two equations are obtained. Subtracting the 2 equations yields a relation representing the height correction to the standard height in ISA conditions caused by a constant ISA deviation ΔISA:

$$\Delta h_{correction} = \frac{\Delta ISA}{\lambda} \cdot \ln\left(1 + \frac{\lambda(h - h_a)}{T_{a,ISA}}\right) \tag{11}$$

Note that equation (11) is exactly formula (2) given in PANS-OPS Volume II, except that the sign is reversed as PANS-OPS considers the correction to be applied to the minimum safe altitude rather than to the aircraft altitude (that means minimum safe altitudes must be raised in case of cold temperature which means a positive correction for a negative ISA deviation). Note that this formula is theoretically an approximation as we have assumed constant temperature profiles with height when integrating equation (9). In addition, the formula assumes standard pressure at airport elevation (which practically means that the QNH is 1013.25 hPa).

A theoretically more correct formula that also allows computing height corrections in case of non-standard temperature lapse rates, can be obtained starting back from equation (8), assuming that the

temperature profile varies with the height above ground h_g. In that case, equation (8) can be rewritten as follows:

$$\frac{1}{\lambda}\cdot\ln\left(\frac{T_0+\lambda h}{T_0}\right)+\frac{R}{g}\ln\left(\frac{p_a}{p_0}\right)=\int_0^{h_g}\frac{1}{T}\cdot\left(\frac{dh_g}{dT}\right)dT \qquad (12)$$

Assuming that the inverse of the temperature lapse rate between the ground and h_g is constant, equation (12) can be integrated which yields the following relation:

$$\frac{dh_g}{dT}=\frac{\frac{1}{\lambda}\cdot\ln\left(\frac{T_0+\lambda h}{T_0}\right)+\frac{R}{g}\ln\left(\frac{p_a}{p_0}\right)}{\ln\left(\frac{T}{T_a}\right)}$$

$$h_g=\frac{\frac{1}{\lambda}\cdot\ln\left(\frac{T_0+\lambda h}{T_0}\right)+\frac{R}{g}\ln\left(\frac{p_a}{p_0}\right)}{\ln\left(\frac{T}{T_a}\right)}\cdot\left(T-T_a\right) \qquad (13)$$

With:

T = actual temperature at pressure height h

T_a = actual temperature at airport elevation

Equation (13) is a generally applicable formula relating the geopotential height h_g above ground to the pressure height h above 1013.25 hPa, the actual airport pressure p_a, the actual airport temperature T_a and the actual temperature T at pressure height h. It is possible to write a few variations to this formula, for example assuming a non-standard temperature variation with pressure height above airport elevation h_a:

$$T=T_a+\lambda'\Delta h \qquad (14)$$

With:

λ' = non-standard temperature lapse rate

$\Delta h = h - h_a$ = pressure height - airport elevation

In this case, equation (13) could be written as:

$$h_g=\frac{\frac{1}{\lambda}\cdot\ln\left(\frac{T_{a,ISA}+\lambda\Delta h}{T_0}\right)+\frac{R}{g}\ln\left(\frac{p_a}{p_0}\right)}{\ln\left(1+\frac{\lambda'\Delta h}{T_a}\right)}\cdot\lambda'\Delta h \qquad (15)$$

Finally, if the pressure at airport elevation is the standard pressure ($p_a = p_{a,ISA}$), equation (15) simplifies to:

$$h_g=\frac{\frac{1}{\lambda}\cdot\ln\left(1+\frac{\lambda\Delta h}{T_{a,ISA}}\right)}{\ln\left(1+\frac{\lambda'\Delta h}{T_a}\right)}\cdot\lambda'\Delta h \qquad (16)$$

Note that if a constant ISA deviation is considered ($T_a = T_{a,ISA} + \Delta$ISA and $\lambda' = \lambda$), equation (11) gives results that are very similar to equation (16). For an ISA deviation of 30 degrees and an airport at sea level, the difference in h_g between both formulas ranges from 0ft on the ground to 24ft at 35000ft. Note also that all formulas given in this chapter apply only below the tropopause.

Discussion of Results

The purpose of the tests was not to compare performance of individual aircraft with each other. Therefore in the discussion of the results, the aircraft types will be further indicated as A/C 1, A/C 2 up to A/C 5, whereby the number corresponding to a particular aircraft type was randomly chosen.

The first step of the post analysis consisted in determining the exact temperature profile that existed in the simulator during each simulator run. The ISA deviation at airport elevation was recorded before each run. The lapse rate was obtained either by recorded data from the simulator, which for some aircraft contained a temperature reading at each recorded altitude, or alternatively it was derived from the Indicated and True Airspeed which was available for all aircraft (either through recorded data or video).

Knowing the exact temperature profile and the recorded pressure altitudes (either from recoded data or video), the geopotential heights were calculated using the exact formulas (16) or (10) for all simulator runs at the following points:

- Distance to threshold at which final approach course (localizer) was captured
- Distance to threshold at which the glide path was captured
- Distance threshold at which the aircraft crossed the Final Approach Point

Next, the geopotential altitude was compared with the pressure altitude at the distance to threshold where the aircraft crossed the FAP and a representative ISA deviation was computed using the PANS-OPS Volume II formula given by equation (2). This representative ISA deviation would result in the same height difference between geopotential and pressure height at the FAP, in case the ISA deviations were constant with altitude.

The complete list of scenarios flown in the 5 aircraft simulators is presented in the Scenario Table in the Appendix. The columns in this table present the following parameters for the 5 aircraft types:

- Scn. No.: the scenario reference number
- FAP Dist. (NM): distance to threshold of the FAP location
- G/S (°): the applied glide path angle of the final approach
- VNAV Path (°): the angle defined by the altitude constraints at start and end points of the RF turn
- Wind: applied wing in the simulator; note that the landing runway direction was 081°
- Bias (NM): magnitude of the simulated lateral navigation error (>0 if the bias led to an undershoot of the localizer, <0 if the bias led to an overshoot of the localizer)
- ΔISA (°C): the representative ISA deviation at the FAP
- G/S Capture (manual/auto): indicates whether flight crew intervention was required to capture the glide path; auto if glide was captured just by arming the approach mode, manual if corrective action by the flight crew to the aircraft's path was necessary to capture the glide
- Ta (°C): temperature at airport elevation (1486ft)
- Gamma' (°C/ft): temperature lapse rate with pressure altitude

For 3 out of the 5 aircraft types, full data recordings were available including the geopotential aircraft height and the aircraft's horizontal position versus time. Figures 9 to 14 illustrate the recorded lateral and vertical profiles for aircraft 1, 2 and 3, for the intercepts of a 3 degree glide path at 6NM from the threshold. The reference procedure consisting of a 2 degree barometric descent path, transitioning to a 3 degree glide path at 6NM is indicated by the black dashed line in the vertical plots.

The vertical profiles for aircraft 1 (see Figure 12) indicate that for a below ISA temperature profile (ISA-37), the aircraft was originally below the desired path but reaching the FAP altitude, a level off was made after which the aircraft correctly intercepted the glide path at about 5NM from the threshold. An above ISA deviation (ISA+31) caused no difficulties during scenario RF14 to capture the glide path, but a similar ISA deviation (ISA+28) led to a corrective action by the flight crew and a glide path interception from above during scenario RF6. If the lateral profiles of RF14 and RF6 are compared (see Figure 9), it turns out that RF6 had a lateral navigation error in addition to the high temperature, causing the aircraft to undershoot the localizer. This indicates that, besides the temperature deviation, the lateral navigation accuracy has an impact on the capability to correctly intercept the glide path at the desired FAP location.

The vertical profiles for aircraft 2 (indicated in Figure 13) look very consistent, independent from the applied lateral navigation error which can be observed in Figure 10. This is because this aircraft could cope better with lateral navigation errors while intercepting the final approach course, which is also obvious in Figure 10. Both high and low temperature deviations (ISA+33 and ISA-37) caused no difficulties in intercepting the glide path at the FAP, located 6NM from the threshold.

Finally, the vertical profiles for aircraft 3 are displayed in Figure 14. The vertical profile of scenario RF5 containing a below ISA deviation (ISA-33) is as expected: the aircraft performs a level off when reaching the FAP altitude and captures the glide path exactly at the FAP altitude, approximately 1NM beyond the 6NM FAP location. An inconsistency can be seen between the vertical profiles of scenarios RF2 and RF4 and scenarios RF 1, RF3 and RF9, all containing above ISA deviations (ISA+29). This can be explained by the fact that a different vertical guidance mode was engaged in the aircraft during the descent along the RF leg. In

scenarios RF1, RF3 and RF9, the flown vertical path corresponds well with the designed 2 degree barometric descent path. Due to the above ISA deviation (ISA+29), the aircraft arrived above the FAP height at the FAP location which led to a short flight crew intervention, capturing the glide path slightly from above. During scenarios RF2 and RF4, a flight mode was engaged which instead of flying a constant barometric flight path angle between the two programmed altitude constraints, gave priority to decelerating the aircraft before the crossing the FAP location. As a consequence the aircraft made a short level off before the FAP which resulted in a glide path interception without requiring flight crew intervention. Also, this aircraft could cope very well with the lateral navigation errors while intercepting the final approach course (see Figure 11) so that these lateral navigation errors did not have much effect on the vertical capture.

Figures 15 to 20 illustrate the recorded lateral and vertical profiles containing a steeper glide path for aircraft 1 and aircraft 3.

Figure 18 displays the data obtained from aircraft 1 for three different procedures: a 4 degree glide path interception from respectively a 2 degree and a 3 degree barometric descent at 3NM from the threshold and a 4.5 degree glide path interception from a 2 degree barometric descent at 6NM from the threshold. The reference path for these 3 procedures is displayed by a dashed line. All three scenarios were flown with an above ISA deviation (ISA+30) and without lateral navigation error. While the interception of the 4 degree glide path at 3NM from the 2 degree barometric descent caused no problems the same glide path interception at the same FAP location but from a 3 degree barometric descent caused a significant overshoot of the glide path, requiring manual intervention from the flight crew. The latter scenario only intercepted the glide path at 1.5NM from the threshold at about 600ft above ground, which is unacceptable. The scenario which was supposed to intercept the 4.5 degree glide path never even capture the glide, as the aircraft arrived above the FAP height and the flight crew was not able to adjust the situation. This indicates that the scenario containing a glide path of 4.5 degrees, starting at only 3NM from the threshold was too challenging.

Figure 19 displays the vertical profiles flown by aircraft 3, which were supposed to intercept a 4 degree glide from a 2 degree barometric descent at 6NM from the threshold. Again a variation in barometric descent behavior can be observed which is related to the engaged vertical guidance mode in this aircraft. Interestingly there are two scenarios, RF14 and RF15, which were flown with an above ISA deviation (ISA+27) and for which a significant flight crew intervention was required to capture the glide from above. These are the scenarios containing besides the above ISA deviation, a lateral navigation error causing the aircraft to undershoot the final approach course (localizer). This again shows the impact of the lateral navigation errors on the vertical capture capability and performance.

Finally, Figure 20 illustrates the vertical profiles of aircraft 3 for the 4 degree glide path intercepts from a 2 degree barometric descent at 3NM. Although scenario RF20, containing an above ISA deviation (ISA+30), originally descents below the barometric path and crosses the glide from a level position, it still overshoots the glide, after which a flight crew correction is made to intercept the glide at only 2NM from threshold. The reason for the aircraft not capturing the glide automatically is again the fact that there was besides the high temperature, a lateral navigation error causing the aircraft to undershoot the final approach course.

Another issue with steep glide paths is the fact that the outside visual cues, as well as the flaring technique during landing are different. Figure 21 shows an aircraft on short final while on a 4 degree glide path, with four white lights on the PAPI.

Figure 21. Outside View of Short Final with 4° glide and 4 white lights on PAPI

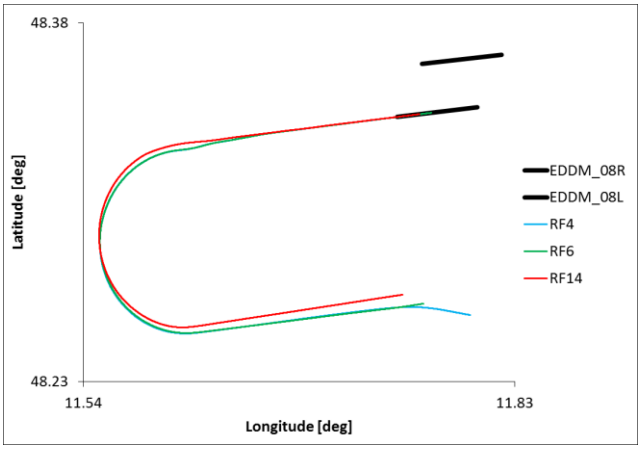

Figure 9. A/C 1 Lateral Profiles for 3° Glide Intercepts at 6NM

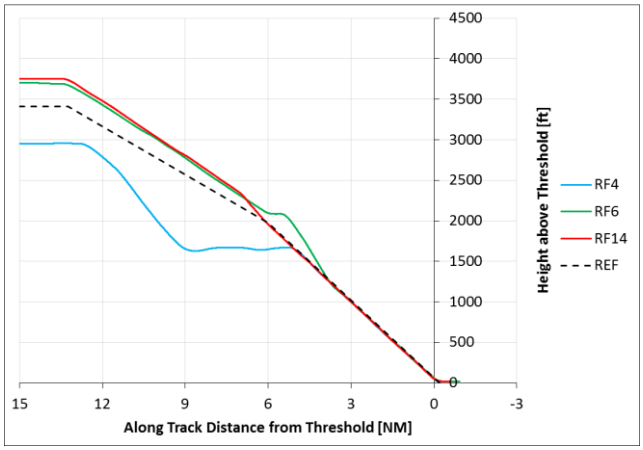

Figure 12. A/C 1 Vertical Profiles for 3° Glide Intercepts at 6NM

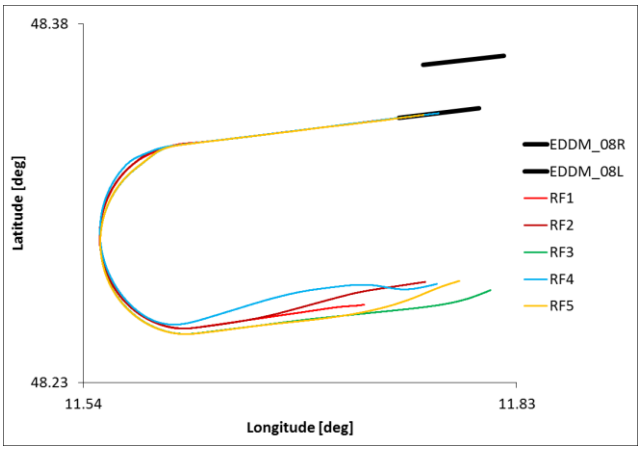

Figure 10. A/C 2 Lateral Profiles for 3° Glide Intercepts at 6NM

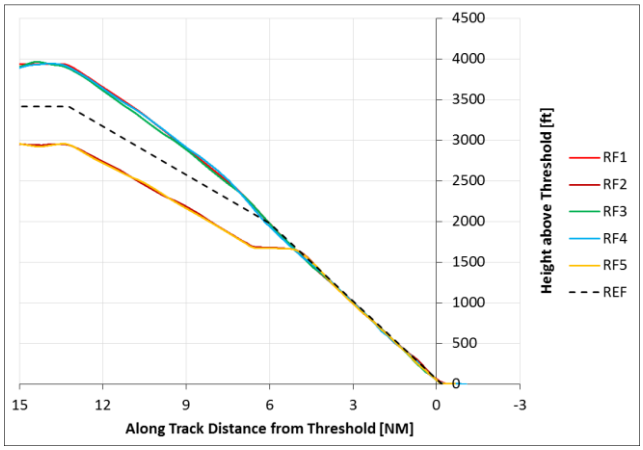

Figure 13. A/C 2 Vertical Profiles for 3° Glide Intercepts at 6NM

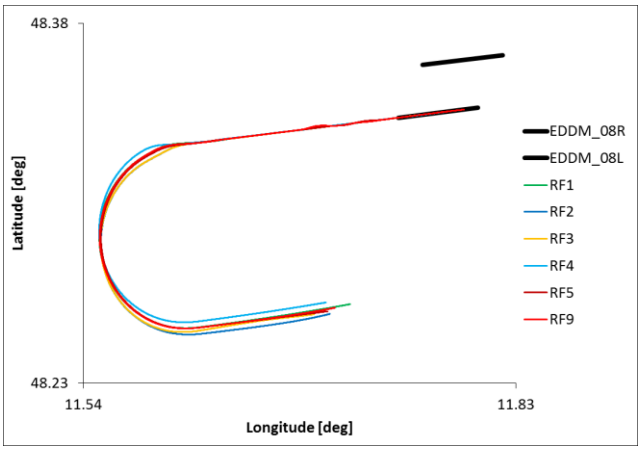

Figure 11. A/C 3 Lateral Profiles for 3° Glide Intercepts at 6NM

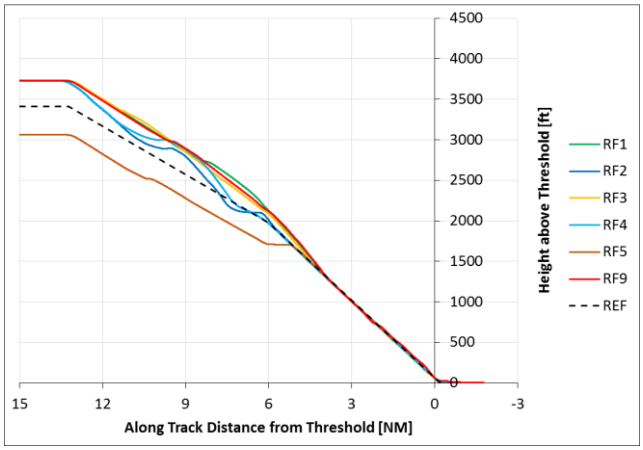

Figure 14. A/C 3 Vertical Profiles for 3° Glide Intercepts at 6NM

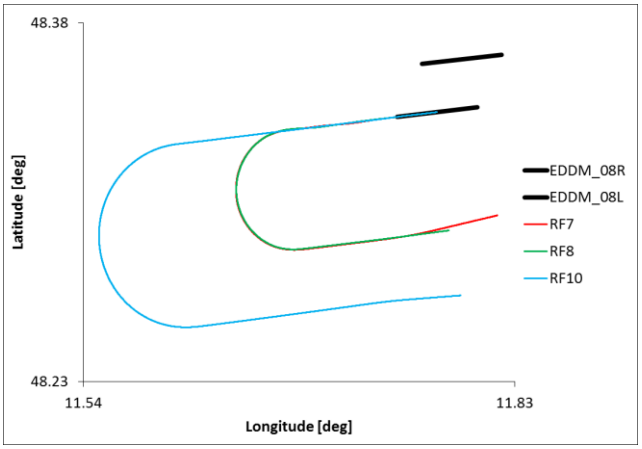

Figure 15. A/C 1 Lateral Profiles for 4° Intercepts at 3NM and 4.5° Intercepts at 6NM

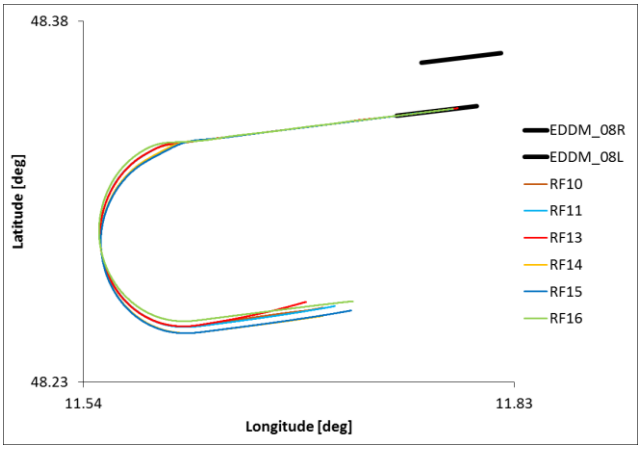

Figure 16. A/C 3 Lateral Profiles for 4° Glide Intercepts at 6NM

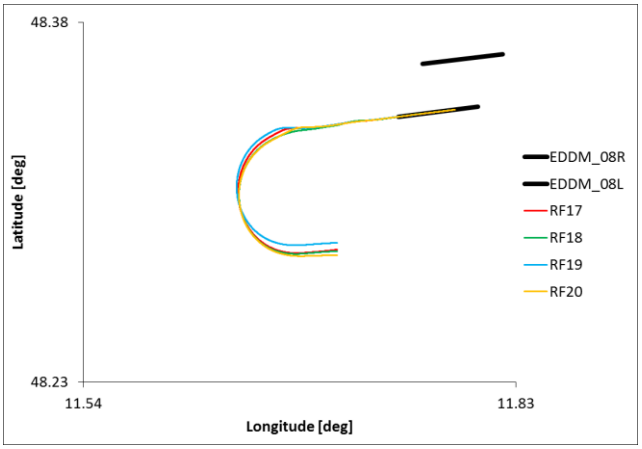

Figure 17. A/C 3 Lateral Profiles for 4° Glide Intercepts at 3NM

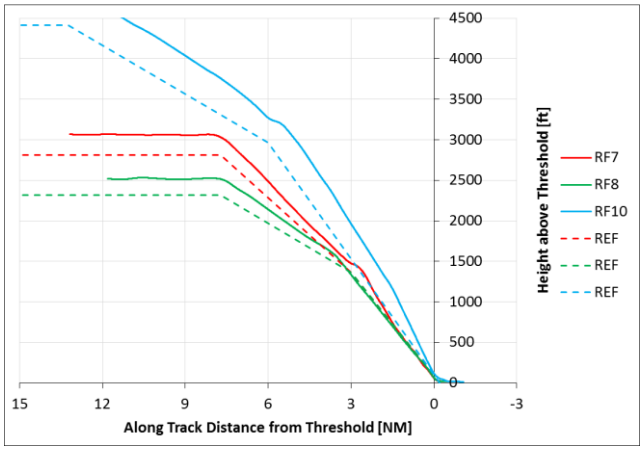

Figure 18. A/C 1 Vertical Profiles for 4° Intercepts at 3NM and 4.5° Intercepts at 6NM

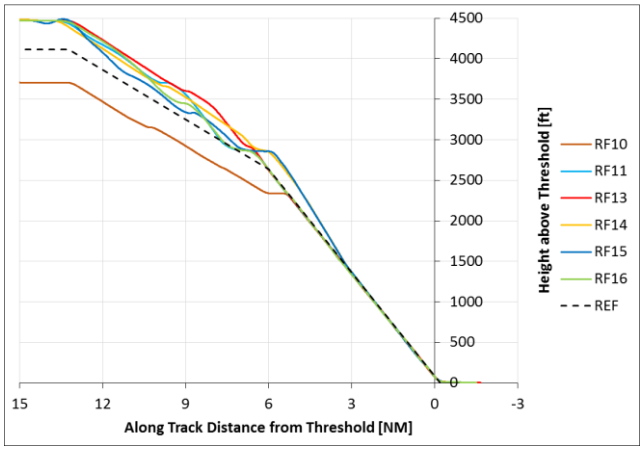

Figure 19. A/C 3 Vertical Profiles for 4° Glide Intercepts at 6NM

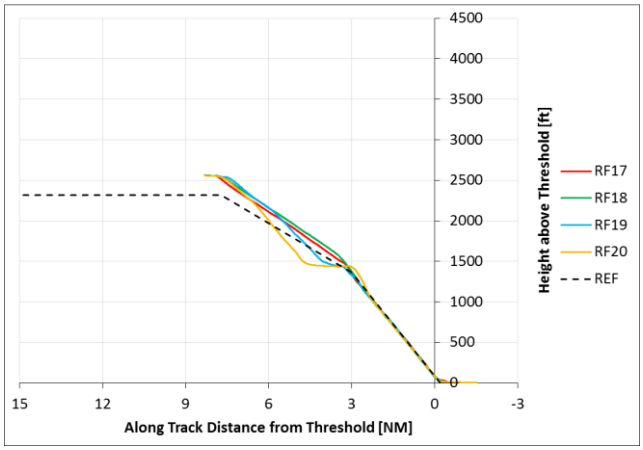

Figure 20. A/C 3 Vertical Profiles for 4° Glide Intercepts at 3NM

Figure 22 provides an overview of the recorded or calculated geopotential heights of the aircraft when crossing the FAP for the scenarios intercepting a 3 degree glide at 6NM. Figure 23 provides the same information for the scenarios intercepting a 4 degree glide both at a 3NM and a 6NM FAP. The dots on both figures are color coded: a full red dot means that flight crew intervention was necessary to intercept and capture the glide path. A hollow green dot means that glide path capture was possible without flight crew intervention other than arming the approach mode and standard aircraft configuration for approach and landing. The dashed lines in Figure 22 and 23 represent the half-scale glide path deviation, assuming that the half-scale glide path angular sector width has the recommended value of 12% of the glide path angle both above and below the glide path centerline, as described in [15]. As expected, the dots in Figures 22 and 23 which are above the glide path centerline (but still within the half scale deviation) are mostly in red, which means that the aircraft arrived above the designed FAP crossing height and flight crew intervention was necessary to increase the descent angle and capture the glide from above.

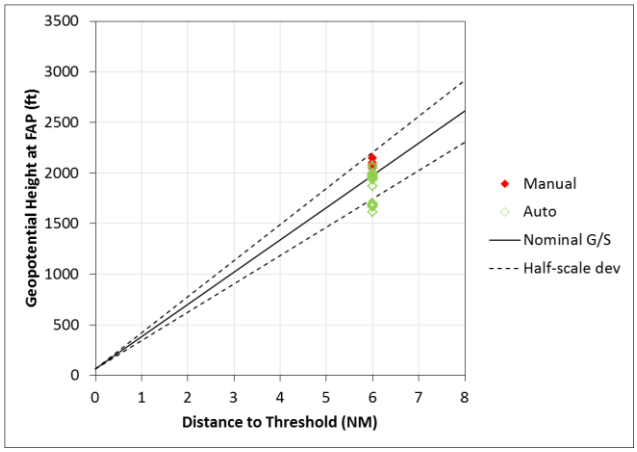

Figure 22. Crossing Height at FAP for 3° Glide Intercepts

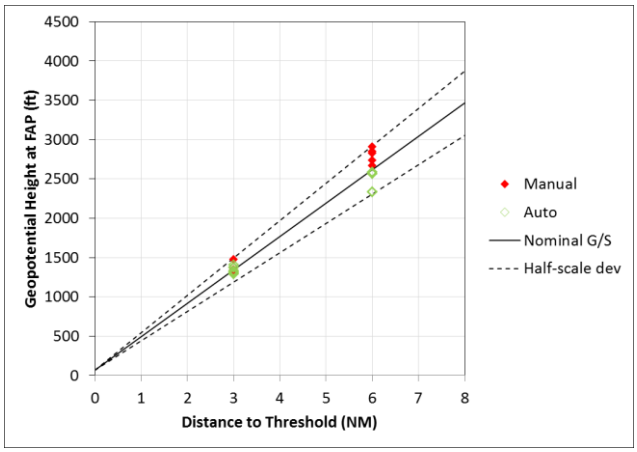

Figure 23. Crossing Height at FAP for 4° Glide Intercepts

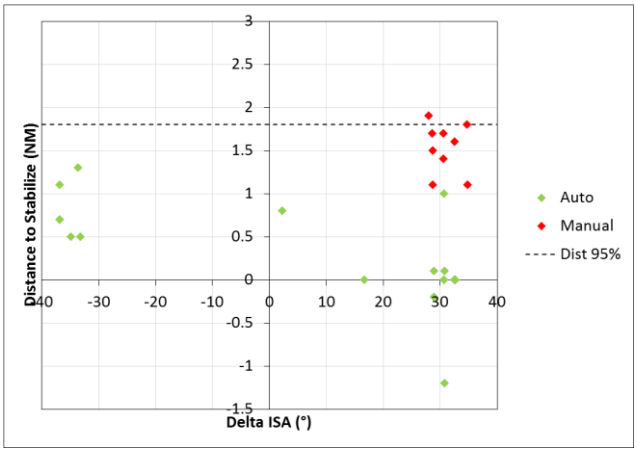

Figure 24. Distance from FAP to Stabilize versus ISA Deviation for 3° Glide Intercepts

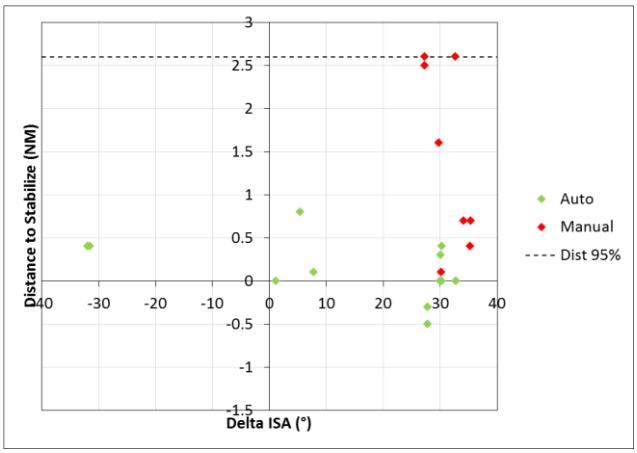

Figure 25. Distance from FAP to Stabilize versus ISA Deviation for 4° Glide Intercepts

Figures 24 and 25 present the measured distance from the FAP towards the threshold which was required to stabilize the approach, in function of the representative ISA deviation at the FAP, for respectively the 3 degree and 4 degree glide path intercepts. Conditions for which the aircraft is considered stable were defined exactly the same as in [5], i.e. both LOC and G/S modes engaged and deviations within one dot, aircraft track converging to its final state and within 5 degrees of the LOC course, no excessive rate of descent and speed corresponding to the distance to threshold and aircraft configuration. The dots in figures 24 and 25 are also color coded depending on whether glide slope capture was with (red) or without (green) flight crew intervention. Obviously the red dots in Figures 24 and 25 are all on the right hand side of the figure, corresponding with the high, positive ISA deviations. Exactly these scenarios also generated the longest distance to stabilize. For the 3 degree glide path intercepts, as indicated in Figure 24, the 95% boundary of the distance to stabilize is 1.8NM (measured from the FAP to the threshold). This corresponds well with the earlier conclusion formulated in [5], i.e. that for procedure designs without an intermediate segment, 5NM from the threshold should be the closest location of the FAP, in order to have the aircraft fully stabilized at 3NM (corresponding for a 3 degree glide to approximately 1000ft). The 95% boundary of the distance to stabilize for the 4 degree glide path intercepts, according to Figure 25, is 2.6NM. This means that a steeper glide path requires more distance from the FAP towards the threshold to get the aircraft fully stable. Thus ideally, the FAP for a steeper glide path should be somewhat further from the threshold than the FAP for a nominal 3 degree glide path.

Figures 26 to 28 provide the geopotential heights versus distances to threshold of the position where the localizer and glide path were captured, for respectively the 3 degree glide intercepts at 6NM, the 4 degree glide intercepts at 6NM and the 4 degree glide intercepts at 3NM. Again, the half scale glide path deviations are indicated by dashed black lines, whereas the nominal glide path is indicated by a solid black line. The dots are again color coded: green means that the glide path was intercepted without flight crew intervention while red means that flight crew intervention was necessary, usually to capture the glide path from above. Because of the above definitions, the dots corresponding to one scenario, representing the localizer intercept and the glide path intercept for that scenario, always have the same color as it is the glide path intercept behavior that determines the color coding.

Figure 26 clearly indicates that there is a relation between the distance at which the localizer was intercepted and whether the glide path was captured automatically or through flight crew intervention. The green dots on the upper right side of the figure are mostly scenarios with high ISA deviations, but because the localizer was intercepted early (well before the FAP) and because the aircraft was still flying the 2 degree barometric descent path at that moment, the glide path capture caused no problems. In many of these “early” localizer capture scenarios, glide path and localizer capture occur simultaneously. Most red dots representing localizer capture are in the vicinity of the FAP for procedures with high positive ISA deviations. The corresponding red dots representing glide path capture are much further down the glide path and well beyond the FAP, which means that the flight crew had to capture the glide from above. Note that all glide path deviations were still within half-scale deflection during this operation. Also interesting to observe is that the scenarios with below ISA deviations are all in green, as the aircraft leveled off during or just after localizer capture and then captured the glide just beyond the FAP from the height at which it had leveled off.

Similar conclusions can be drawn from Figure 27 except that in this case, almost all above ISA deviations required flight crew intervention to capture the glide path. This suggests that in case of high positive ISA deviations, capturing a steeper glide is even more difficult than capturing a nominal 3 degree glide path. Also it can be seen from Figure 27 that it takes more distance for the flight crew to correct in case of glide capture issues. Some glide captures only occur at 3.5NM from the threshold, which is 2.5NM beyond the FAP.

Also in Figure 28, it can be seen that for one scenario with above ISA conditions, localizer intercepts occurs well before the FAP al 3.8NM, but because of the steep glide, it takes about 2.5NM more to capture the glide path at only 1.3NM from the threshold, which is unacceptable.

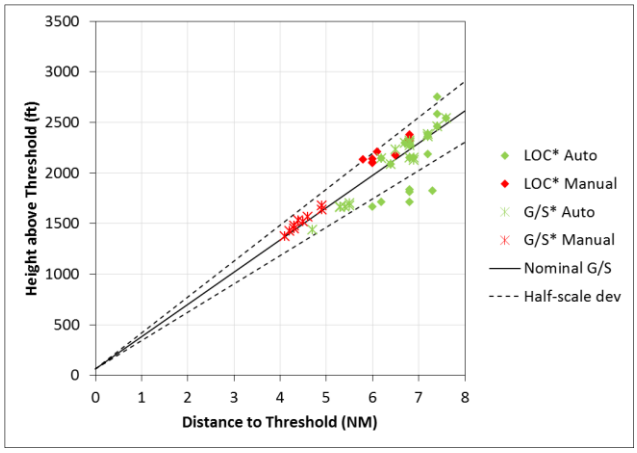

Figure 26. LOC and G/S Capture Points for 3° Glide Intercepts at 6NM

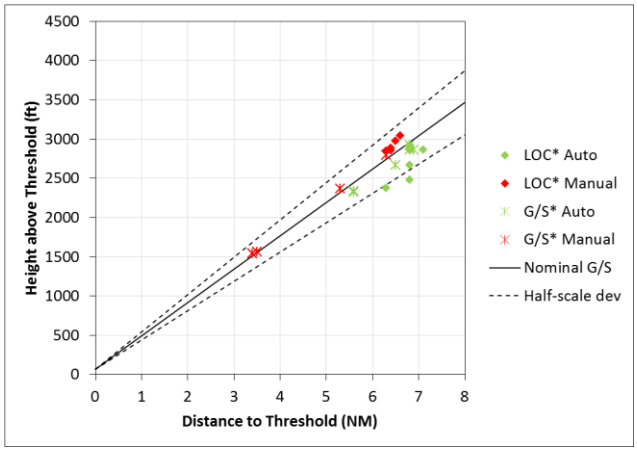

Figure 27. LOC and G/S Capture Points for 4° Glide Intercepts at 6NM

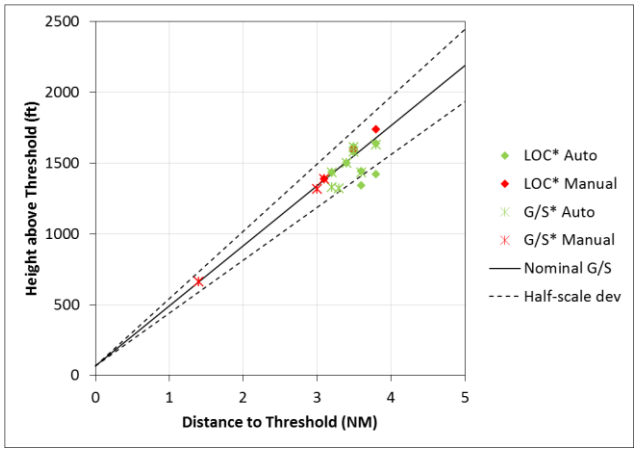

Figure 28. LOC and G/S Capture Points for 4° Glide Intercepts at 3NM

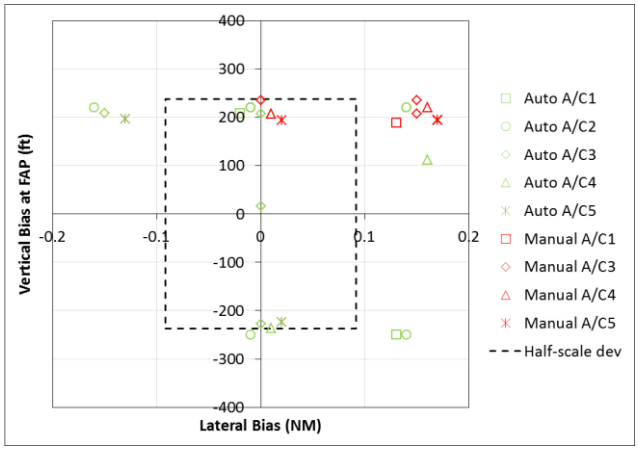

Figure 29. Lateral versus Vertical Bias at FAP for 3° Glide Intercepts at 6NM

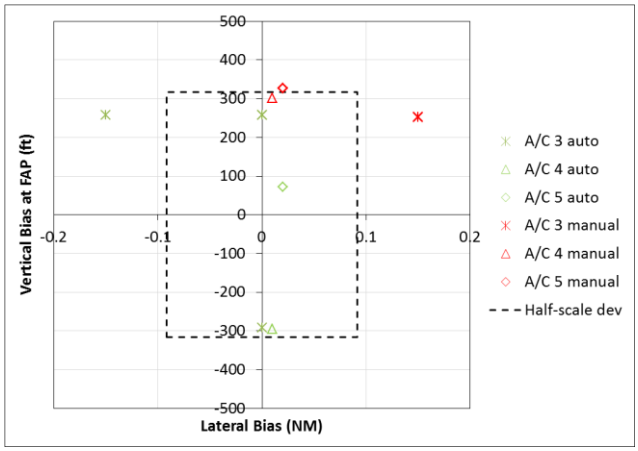

Figure 30. Lateral versus Vertical Bias at FAP for 4° Glide Intercepts at 6NM

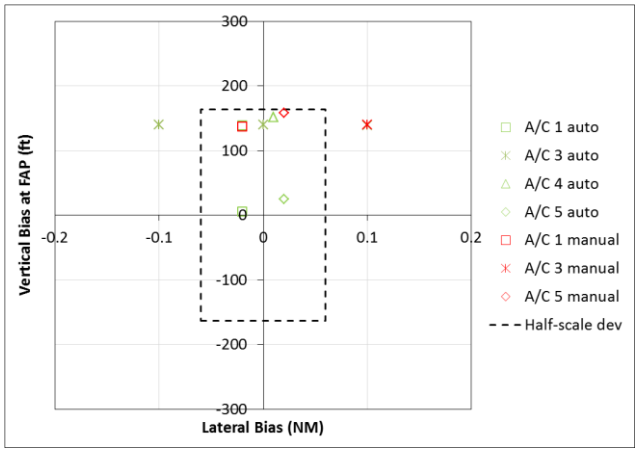

Figure 31. Lateral versus Vertical Bias at FAP for 4° Glide Intercepts at 3NM

Figures 29 to 31 provide a combined overview of the lateral and vertical navigation biases introduced in each simulation and for each aircraft type, respectively for the 3 degree glide intercepts at 6NM, the 4 degree glide intercepts at 6NM and the 4 degree glide intercepts at 3NM. The vertical navigation biases are equal to the height correction given by formula (2) resulting from the representative ISA deviation at the FAP for each scenario. The dashed box in Figures 29, 30 and 31 represents the half-scale deflections of the localizer and glide path at the FAP. Different symbols are used for each aircraft type and again, the symbols are color coded as follows: green for scenarios which did not require flight crew intervention to capture the glide and red for scenarios which required flight crew intervention to capture the glide path (usually from above).

Some general trends can be observed from Figures 29, 30 and 31. First of all, the introduced ISA deviations (between ISA-37 and ISA+35) caused aircraft height biases within one half-scale glide path deviation at the FAP. Below ISA deviations never caused any problems capturing the glide path. For some aircraft types, high positive ISA deviations without lateral navigation errors required flight crew intervention to capture the glide. For all aircraft types except one, high positive ISA deviations in combination with a lateral navigation error causing the aircraft to undershoot the localizer, required flight crew intervention to capture the glide.

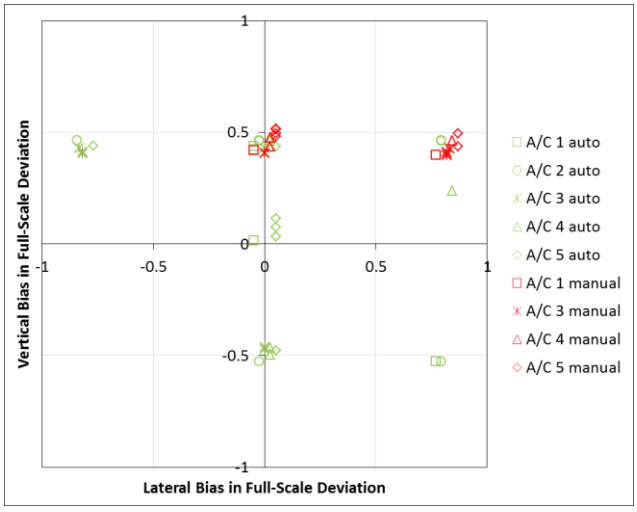

Figure 32. Lateral versus Vertical Bias at FAP for all scenarios (3°, 4°, 3 NM and 6NM)

Finally Figure 32 provides a collective overview of all scenarios, displaying the vertical bias at the FAP caused by temperature and expressed in units of full scale deviation on the glide path, versus the lateral bias expressed in units of full scale deviation on the localizer. Each aircraft is represented by a different symbol using the same color coding as before. The same overall conclusion can be drawn as for Figures 29 to 31.

Procedure design options

The same observations as for the simulation results can be made intuitively when analyzing the procedure design and the effects of lateral and vertical deviations caused by temperature on the aircraft's position relative to the glide path and localizer half-scale or full-scale deviations and glide path coverage area.

Figure 33 illustrates the PBN procedure in red with the assumed maximum lateral deviations displayed by the red dashed line. If the assumed maximum lateral deviation is +/- 0.16NM (which is realistic for modern equipment using GNSS) the aircraft will exactly arrive within the localizer full scale deviation (indicated by the black dotted line) at 5NM from the threshold. Note that in this design a localizer full scale angular width of 2.41 degrees is assumed with the localizer antenna situated 4981m beyond the threshold as in [5]. Figure 33 also illustrates the glide path coverage area by the black dashed line, defined in [15] as 8 degrees in azimuth on each side of the centerline of the ILS glide path. It can be seen that for this particular design, i.e. a localizer intercept at 5NM from a circular PBN path with a 2.3NM radius, the glide path will already be visible to the pilot at about 7NM from the threshold, as the PBN path crosses the glide path coverage area boundary at this distance.

Figure 34 illustrates a 3 degree nominal glide path as well as the glide path half-scale deviation area, indicated by the black dashed line. Note that [15] allows some variation of the glide path half-scale sensitivity. For ILS CAT II/III installations, nominal angular displacement sensitivity shall correspond to a half ILS glide path sector at an angular displacement of 0.12 θ below path with a tolerance of plus or minus 0.02 θ (with θ denoted as the slope of the glide path). For ILS CAT I

installations, the same values are recommended and the angular displacement sensitivity should be as symmetrical as practicable around the glide path centerline. For GBAS, the glide path displacement sensitivity is equivalent to the one provided by a typical ILS [15]. In Figure 34, the angular width of the half-scale glide path displacement is set to 0.12 θ. In addition, a solid red line indicates a 2 degree barometric descent path connecting to the glide at 5NM, in function of the distance to threshold measured parallel to localizer centerline. Note that there are two points on the red line corresponding to each distance greater than 5NM, which is due to the fact that this section of the vertical path lies on the lateral circular arc of the PBN procedure. The dotted red lines show the resulting vertical path in case the aircraft would fly the same barometric 2 degree path in respectively ISA+34 and ISA-34 temperature conditions. In the latter cases, the aircraft would exactly arrive at the half-scale xLS glide path deviation at 5NM from the threshold. At 8NM from the threshold, when the glide path becomes visible to the pilot (according to Figure 33), the aircraft would be slightly below glide path in ISA conditions and at about 1/4th of the full scale deviation above the glide path in ISA+34 conditions. Moreover if the aircraft flies the nominal lateral path, it can be seen in Figure 33, that it would enter the localizer full-scale deviation area at about 6NM. Figure 34 indicates that at this position, the aircraft is still well below the upper half-scale glide path deviation. This is operationally a perfectly acceptable situation, provided that there is still some distance to go for the pilot to get the glide path indication fully centered.

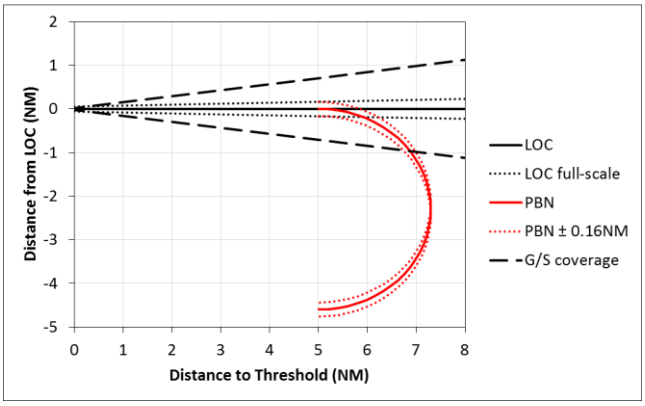

Figure 33. RF Turn to FAP at 5NM with LOC Full Scale and Glide Coverage Areas

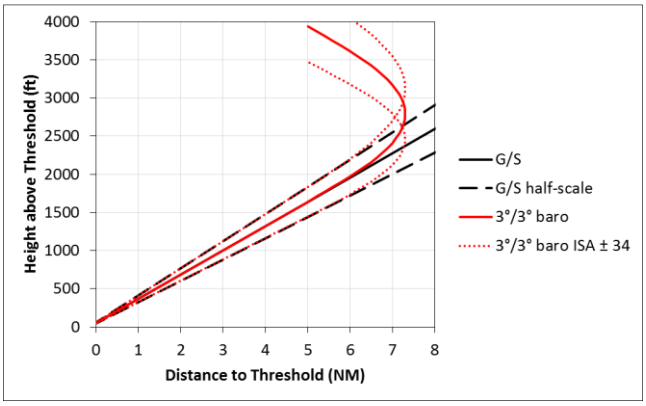

Figure 35. 3° Descent Along RF Leg Connected to 3° Glide at 5NM

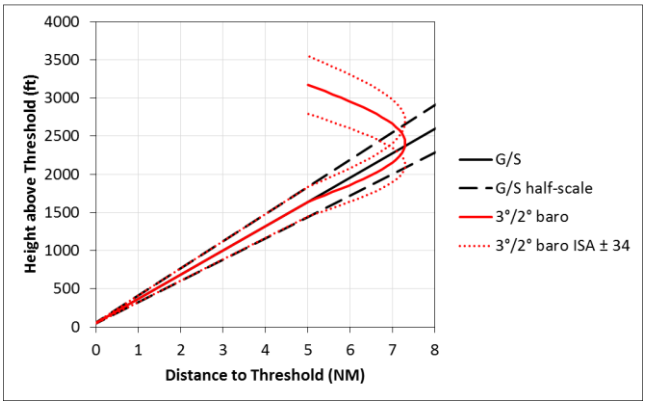

Figure 34. 2° Descent Along RF Leg Connected to 3° Glide at 5NM

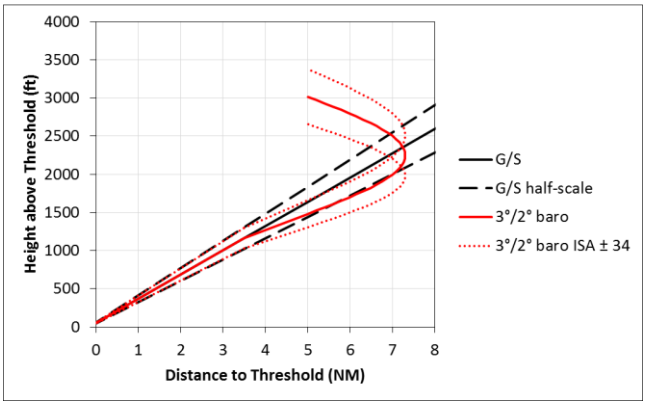

Figure 36. 2° Descent Along RF Leg + 1.5NM Straight Segment Connected to 3° Glide at 3.5NM

Figure 35 illustrates the same design as in Figure 34, except that the barometric descent angle is 3 degrees instead of 2 degrees. Immediately it can be seen that in case of an ISA+34 temperature deviation, the aircraft will always have to intercept the glide path from above the half-scale deviation.

Finally, Figure 36 illustrates a more conventional design, whereby the final approach course is still intercepted at 5NM, as depicted in Figure 33, but the glide path interception is at 3.5NM. Between localizer and glide path interception is a 1.5NM intermediate segment aligned with the final approach course. The vertical design in Figure 36 is such that the aircraft flies a 2 degree barometric descent all along the RF leg and the 1.5NM intermediate segment, after which it transitions to a 3 degree glide path. In this case, the aircraft will arrive at the 5NM localizer intercept point at one half-scale deviation below the glide path in ISA conditions and exactly on the glide path in ISA+34. Therefore it can be expected that with this design, the glide path interception could be performed without any flight crew intervention in the vertical dimension (other than arming the approach mode), for all considered ISA deviations. The drawback might be that the glide path will be intercepted from a lower altitude, compared to the case presented in Figure 34 where both glide path and final approach course are intercepted at 5NM.

Conclusions

Flight simulations have been performed using 5 different professional flight crew training simulators, investigating the combined effect of lateral navigation errors and non-standard temperature profiles on the transition from a curved PBN procedure (using RF leg functionality) to an xLS final approach. The vertical navigation errors ranged from -0.15NM to +0.15NM while the temperature offsets at the Final Approach Point (FAP) varied between ISA-37 and ISA+35.

Analysis of the simulations results and the procedure designs has shown that the transition from the RF leg to the xLS final approach, whereby the final point of the RF leg is connected directly to the Final Approach Point (FAP) of the xLS procedure, is possible. This is true under certain conditions which are as discussed further below.

The FAP should be located at a sufficient distance from the threshold. In [5], a minimum distance of 5NM was proposed assuming lateral navigation errors not greater than those given by equation (1). This can be confirmed by the current results for the nominal glide paths. In case of temperature deviations up to ISA+35, the simulations containing a FAP at 5NM and a 3 degree glide path, required an extra distance of up to 2NM between FAP and threshold to get the aircraft fully stabilized at 3NM (1000ft), which is operationally acceptable.

The vertical path of the aircraft along the PBN procedure should have a significantly shallower slope than the glide path starting at the FAP. In the simulations scenarios presented here, the PBN procedure was bounded by two altitude constraints defining a 2 degree barometric descent path before glide path interception.

Below ISA deviations did not cause issues capturing the glide path as the aircraft levelled off at the FAP altitude and captured the glide path from below. For the scenarios with high positive ISA temperature deviations, especially if these were combined with lateral navigation errors causing the aircraft to undershoot the localizer, flight crew interventions were often required to intercept the glide path. In the latter case the glide path was captured from above, although deviations were within half-scale in case of correct flight crew action and for temperatures up to ISA+34.

Steeper glide paths up to 4 degrees were also tested. In general the same observations as for the 3 degree glide paths are applicable although more distance (2.5NM) between FAP and threshold was required to get the aircraft stable and the rate of crew interventions to capture the glide was slightly higher than in the nominal glide path case.

Finally, a more conventional procedure design was discussed consisting of a final approach path intercept at 5NM, followed by a straight intermediate segment and a glide path intercept at 3.5NM. This procedure was not simulated but analysis of the design estimated that a 2 degree barometric descent transitioning to a 3 degree glide path at 3.5NM would not require flight crew intervention in case of temperature deviations up to ISA+34.

References

[1] RTCA Special Committee 227 and EUROCAE Working Group 85, 2013, DO-236C ED-75C Minimum Aviation System Performance Standards: Required Navigation Performance for Area Navigation.

[2] Herndon, Albert A., Michael Cramer, Kevin Sprong, 2008, Analysis of Advanced Flight Management Systems (FMS), Flight Management Computer (FMC) Field Observations Trials, Radius-To-Fix Path Terminators, St. Paul, Minnesota, 27th DASC.

[3] de Leege, Arjen, Gustavo Mercado, 2011, Radius to Fix Track-keeping Analysis, Report to EUROCONTROL, The Hague, The Netherlands, To70.

[4] SESAR WP6.8.8, Enhanced Arrival Procedures Enabled by GBAS - Operational Service and Environment Definition (OSED), 2014, SESAR Joint Undertaking.

[5] De Smedt, David, Emilien Robert, Ferdinand Behrend, 2014, RNP to Precision Approach Transition Flight Simulations, Colorado Springs, Colorado, 33rd DASC.

[6] International Civil Aviation Organization (ICAO), 2013, Doc 9613 Performance-based Navigation (PBN) Manual, Fourth edition, Montreal, Canada, ICAO.

[7] Herndon, Albert, Michael Cramer, Sam Miller, Laura Rodriguez, 2014, Analysis of Advanced Flight Management Systems (FMSs), Flight Management Computer (FMC) Field Observations Trials: Performance Based Navigation to x Landing System (PBN to xLS), Colorado Springs, Colorado, 33rd DASC.

[8] International Civil Aviation Organization (ICAO), 2006, Doc 8168 Volume II Construction of Visual and Instrument Flight Procedures, Fifth edition, Montreal, Canada, ICAO.

[9] Airlines Electronic Engineering Committee (AEEC), 2011, ARINC Specification 424-20 "Navigation System Database", Annapolis, Maryland, Aeronautical Radio Inc.

[10] International Civil Aviation Organization (ICAO), 2006, Doc 8168 Volume I Aircraft Operations, Fifth edition, Montreal, Canada, ICAO, Part III, Section1, Chapter 4.

[11] Transport Canada, 2013, Advisory Circular 500-020, Issue 3, Flight Management System (FMS) Barometric Vertical Navigation (VNAV) Temperature Compensation, Transport Canada.

[12] Engineering Science Date Unit Publication (ESDU), Equations for calculation of International Standard Atmosphere and associated off-standard atmospheres, Item Number 77022 Amendment C, 2008, ESDU.

[13] NASA, U.S. Standard Atmosphere 1976, Technical Report NASA-TM-X-74335, NOAA-S/T-76-1562, 1976, NASA.

[14] National Aerospace Laboratory NLR The Netherlands, De Berekening van Atmosferische Grootheden en van de Vliegsnelheid voor Verkeersleidingsdoeleinden op Vlieghoogten Beneden 20000m, Memorandum VG-77-048 U, 1977, NLR.

[15] International Civil Aviation Organization (ICAO) Annex 10, 2006, Aeronautical Tele-communications Volume I Radio Navigation Aids, Sixth edition, Montreal, Canada, ICAO.

Disclaimer

The activities developed to achieve the results presented in this paper, were created by EUROCONTROL for the SESAR Joint Undertaking within the frame of the SESAR Programme co-financed by the EU and EUROCONTROL. The opinions expressed herein reflect the author's view only. The SESAR Joint Undertaking is not liable for the use of any of the information included herein.

Email Addresses

david.de-smedt@eurocontrol.int

emilien.robert@eurocontrol.int

f.behrend@tu-berlin.de

Appendix: Scenario Table

A/C Type	Scn. No.	FAP Dist. (NM)	G/S (°)	VNAV Path (°)	Wind	Bias (NM)	ΔISA (°C)	G/S Capture	Ta (°C)	Gamma' (°C/ft)
A/C 1	RF4	6	3	2	352/25	0.15	**-37**	auto	-25	-0.0018
	RF6	6	3	2	352/25	0.15	**28**	manual	45	-0.0070
	RF7	3	4	3	calm	0	**30**	manual	45	-0.0068
	RF8	3	4	2	calm	0	**30**	auto	45	-0.0069
	RF9	3	4	2	calm	0	**1**	auto	15	-0.0048
	RF10	6	4.5	2	calm	0	**29**	manual	45	-0.0048
	RF14	6	3	2	calm	0	**31**	auto	45	-0.0044
A/C 2	RF1	6	3	2	calm	0	**33**	auto	45	-0.0023
	RF2	6	3	2	calm	0	**-37**	auto	-25	-0.0018
	RF3	6	3	2	352/25	0.15	**33**	auto	45	-0.0023
	RF4	6	3	2	172/25	-0.15	**33**	auto	45	-0.0023
	RF5	6	3	2	352/25	0.15	**-37**	auto	-25	-0.0018
	RF7	6	3	3	calm	0	**33**	auto	45	-0.0024
	RF8	6	3	3	352/25	0.15	**33**	auto	45	-0.0024
	RF9	6	3	4.5	calm	0	**33**	auto	45	-0.0023
A/C 3	RF1	6	3	2	calm	0	**29**	manual	45	-0.0064
	RF2	6	3	2	352/25	0.15	**29**	auto	45	-0.0064
	RF3	6	3	2	352/25	0.15	**29**	manual	45	-0.0064
	RF4	6	3	2	172/25	-0.15	**29**	auto	45	-0.0064
	RF5	6	3	2	calm	0	**-33**	auto	-25	0.0021
	RF9	6	3	2	calm	0	**29**	manual	45	-0.0064
	RF10	6	4	2	calm	0	**-32**	auto	-25	0.0022
	RF11	6	4	2	calm	0	**28**	auto	45	-0.0063
	RF13	6	4	2	calm	0	**28**	auto	45	-0.0063
	RF14	6	4	2	325/25	0.15	**27**	manual	45	-0.0063
	RF15	6	4	2	325/25	0.15	**27**	manual	45	-0.0063
	RF16	6	4	2	172/25	-0.15	**28**	auto	45	-0.0063
	RF17	3	4	2	calm	0	**30**	auto	45	-0.0065
	RF18	3	4	2	325/25	0.1	**30**	manual	45	-0.0065
	RF19	3	4	2	172/25	-0.1	**30**	auto	45	-0.0065
	RF20	3	4	2	325/25	0.1	**30**	auto	45	-0.0065
A/C 4	RF2	6	3	2	calm	0	**31**	manual	45	-0.0044
	RF3	6	3	2	352/25	0.15	**33**	manual	45	-0.0023
	RF7	6	4	2	calm	0	**-32**	auto	-25	0.0019
	RF8	6	4	2	calm	0	**33**	manual	45	-0.0022
	RF9	3	4	2	calm	0	**33**	auto	45	-0.0022
	RF10	3	4	2	calm	0	**33**	auto	45	-0.0022
	RF1.1	6	3	2	calm	0	**31**	auto	45	-0.0044
	RF4.1	6	3	2	calm	0	**31**	auto	45	-0.0044
	RF5.1	6	3	2	calm	0	**-35**	auto	-25	0.0003
	RF7.1	6	3	2	352/25	0.15	**17**	auto	30	-0.0033
A/C 5	RF0	6	3	2	calm	0	**2**	auto	15	-0.0026
	RF4	6	3	2	calm	0	**31**	auto	45	-0.0044
	RF5	6	3	2	352/25	0.15	**31**	manual	45	-0.0044
	RF6	6	3	2	172/25	-0.15	**31**	auto	45	-0.0044
	RF7	6	3	2	calm	0	**-34**	auto	-25	0.0018
	RF14	6	3	2	calm	0	**35**	manual	45	0.0000
	RF15	6	3	2	325/25	0.15	**35**	manual	45	0.0000
	RF17	6	4	2	calm	0	**35**	manual	45	0.0000
	RF18	6	4	2	calm	0	**35**	manual	45	0.0000
	RF19	3	4	2	calm	0	**34**	manual	45	0.0000
	RF20	3	4	2	calm	0	**5**	auto	15	0.0017
	RF21	6	4	2	calm	0	**8**	auto	15	0.0019